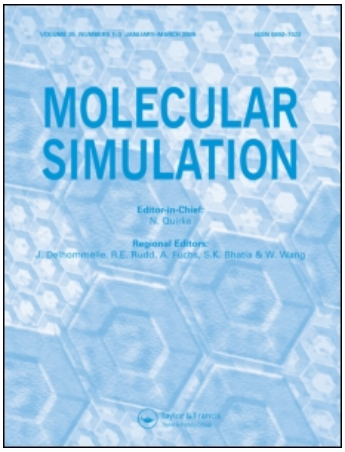

Molecular Simulation
Publication details, including instructions for authors and subscription information:
http://www.informaworld.com/smpp/title~content=t713644482

Molecular Simulation of the Amyloid β-Peptide Aβ-(1-40) of Alzheimer's Disease

Peter P. Mager[a]
[a] Research Group of Pharmacochemistry, Institute of Pharmacology and Toxicology of the University, Saxony, Germany

To cite this Article Mager, Peter P.(1998) 'Molecular Simulation of the Amyloid β-Peptide Aβ-(1-40) of Alzheimer's Disease', Molecular Simulation, 20: 4, 201 — 222
To link to this Article: DOI: 10.1080/08927029808024178
URL: http://dx.doi.org/10.1080/08927029808024178

Molecular Simulation, 1998, Vol. 20, pp. 201–222
Reprints available directly from the publisher
Photocopying permitted by license only

MOLECULAR SIMULATION OF THE AMYLOID β-PEPTIDE Aβ-(1-40) OF ALZHEIMER'S DISEASE

PETER P. MAGER

Research Group of Pharmacochemistry, Institute of Pharmacology and Toxicology of the University, Härtelstr. 16–18, Saxony, Germany

(Received February 1997; Accepted March 1997)

The amyloid Aβ(1-40) peptide of Alzheimer's disease was chosen as model compound. This Aβ peptide is an intrinsically soluble peptide; the C-terminal amino acids are less hydrophilic than the amino acids at the N-terminus, and the degree of hydrophilicity of the N-terminus depends strongly on the *p*H.

The stronger local energy minimum of the random coil and α-helix means that the two conformations are more stable in solution. The relatively high-energy domain of the β-sheet allows to surmount better the energy-barrier height during the formation of an activated complex with polarized ligands and macromolecules. It appears that interactions around the Phe19 and Phe20 area (hydrophobic core) of paired β-sheets play a key role in formatting χ-like filaments. Energy calculation of a bi- and trimer supports the view that the aggregates are energetically stable oligomers which can easily be denatured, however. A perspective in drug research is to develop compounds that stabilize specifically the α-helix and random conformations of Aβ(1-40), or inhibit the hydrophobic core.

Keywords: Morbus Alzheimer; Aβ peptide; molecular simulation; conformation transitions

1. INTRODUCTION

Alzheimer's disease (AD) is a chronic, neurodegenerative disorder which is characterized by pathological brain lesions composed of amyloid deposition [1]. Extracellular deposits consists of amyloid plaques and cerebrovascular amyloid, while intracellular deposits consists of neurofibrillary tangles. The major protein constituent of the deposits is the so-called amyloid β-peptide (Aβ) which is derived from proteolysis of a large (653 to 770 amino acids) transmembrane amyloid precursor protein (APP) by an endosomal/

lysosomal processing pathway [2, 3]. Different spliceforms of APP are encoded by a widely expressed gene. Before a slow formation of a crystallized core, a supersaturated, metastable solution is required. Once the nucleus has formed, growth of the Aβ plaque is fast and thermodynamically favored [4].

Several variants of the naturally occuring Aβ's differing only at the C-terminus (amino acid residues 1-39, 1-40, 1-42, 1-43) are formed by the proteolytic cleavage from the amyloid precursor protein. It appears that the Aβ(1-40) and Aβ(1-42) are the predominant proteins in neuritic plaque while Aβ(1-43) is present as a minor component [5], and Aβ(1-39) is predominant component in cerebrovascular deposits [6]. The Aβ(1-42) and Aβ(1-43) units aggregate more readily than Aβ(1-40), but once aggregated, their relative neurotoxicities appear equivalent under defined experimental conditions. Furthermore, it was demonstrated that freshly prepared random-coil conformation of Aβ(1-40) and Aβ(1-42) are nontoxic or less toxic, while an enhanced neurotoxicity is observed [7] after inducing an aging of a β-sheet conformation by a suitable chemical environment (concentration of the peptide, ionic strength, *p*H, temperature on the one hand, and duration of preparation on the other one).

Unfortunately, experimental studies are problematic once the peptide concentration reaches a critical limit [7, 8]. The ability of cascading β-sheets to form highly anisotropic aggregates ("fibers") renders studies on conformation conversions experimentally very difficult, as also shown by investigating experimentally and theoretically other, more simple peptide models [9–17]. Furthermore, the naturally occuring tertiary structure of proteins is formed along a relatively unknown, "largely mysterious", folding pathway. Due to these two reasons, it should be useful to apply molecular simulation techniques in order to reveal conformation changes of the Aβ (1-40) protein.

2. METHOD

All-atom molecular mechanics (MM) methods [18–20] were used. The MM + empirical potential (force field) is an improved MM2/MM3 version [18, 19]. It was chosen as first method but it does not have an option for changing the dielectric constant ε, in contrast to AMBER force field [20] (Assisted Model Building and Energy Refinement). Correlation-gradient geometry optimization [21] was then achieved. The structures were refined using a conjugate gradient minimizer (Fletcher-Reeves modification of the

Polak-Ribiére method). Convergence was obtained when the gradient root mean square RMS was RMS < 0.07.

The conformations were initially energy minimized using the MM + force field without an electrostatic term. The whole MM + procedure was repeated with electrostatic parameters of an "empirical quantum chemistry module", the connectivity-based iterative partial equalization of orbital electronegativity (Gasteiger method [22]). After including the partial charges, the resulting conformation contained the molecular electrostatic potential and electrostatic energies. Then, the AMBER force field was employed.

To perform explicit solvent simulations, the solvent was treated as a dielectric continuum surrounding the AMBER force field model of the solute molecules after Gasteiger-MM + geometry optimization. In these studies, the following dielectric constans ε were used for AMBER force field calculations (1 atm, 298 Kelvin): $\varepsilon = 1$ (vacuum), $\varepsilon = 3.5$ (lipophilic environment such as membrane-bound proteins, blood-brain barrier, gastrointestinal barriers; $\varepsilon = 2.26$ for benzene, $\varepsilon = 3.38$ for isopropyl ether, $\varepsilon = 4.05$ for chloroform), $\varepsilon = 39.65$ (NaCl solution, 4.0 M NaCl, $\varepsilon = 80$ ($\varepsilon = 78.6$ for pure water, $\varepsilon = 83$ for urine, $\varepsilon = 85$ for blood plasma, $\varepsilon = 85$ to 90 for brain tissue), and $\varepsilon = 130$ (lecithin).

Molecular dynamics calculations were carried out with the Gasteiger-MM + /AMBER geometry-optimized structure in a lecithin-like environment ($\varepsilon = 130$) using the MM + force field. The following options were used: starting time and temperature: 0.1 ps, 100 Kelvin temperature; running time and simulation temperature: 0.5 ps and 600 Kelvin temperature; cooling time and final temperature: 0.5 ps, 0 Kelvin temperature; step size 0.0005 ps.

To investigate the physicochemical properties, the following constants were determined: The distribution coefficients P (octanol/water, neutral microspecies), the pK_a values (at $[K^+] = [Na^+] = [Cl^-] = 0.05$ M; 25°C), the molecular solvent-accessible surface area SA (grid method by adding the solvent radius for water to the van-der-Waals radii), the molar volume MV (grid method), molar refractivity MR, and molecular polarizability Pol (related to MR through the Lorenz-Lorenz equation). The hydration energy ΔH (kcal/mol) is closely related to the stability of different conformations. The determination occurred by computer-aided approaches [29–33] using geometry-optimized structures ($SA, MV, \Delta H$) and simplified molecular identification and line entry system notation ($\log P$, pK_a, MR, Pol). Based on different pH and the pK_a values, the corrected distribution coefficients for ionized agents were calculated by using the Henderson-Hasselbalch equation.

2. RESULTS AND DISCUSSION

Data Source

The primary structure of the complete peptide is given in Table I. The Aβ(1-40) peptide was chosen as model agent due to two reasons. First, it is – beside Aβ(1-42) – the predominant peptide in neuritic plaques. Second, it is relatively easy to work experimentally with it, while Aβ(1-42) aggregates more easily and is virtually impossible to assess chemical purity above the 70% level [8]. The coordinates of Aβ(1-40) peptide were generated from solution NMR data (25 degrees Celsius) and uploaded from the Brookhaven Protein Data Bank [23] (model conformation 2 of the 1AML PDB file, called here A2OPT). As NMR spectroscopy may produce a considerable variability of bond lengths, bond angles, and torsion angles due to the experimental errors, and the resulting structures correspond to one of perhaps many low-energy conformations, geometry optimization was used to improve the geometry data and to get most stable conformers (Tab. II).

The angles of the backbone and residues were randomly varied. Then, reinitiation of an ordered structure was achieved by addition of ordered-structure-enforcing local constraints (torsional angles of the peptide backbone, defining the angles and distances of structure-maintaining hydrogen bonds). The constraints were taken as a function of the degree of structural

TABLE I Sequence of the Aβ(1-43) molecule. The NH_2 and COOH terminal moieties are in 1 and 43 position, respectively. If the studied Aβ(1-40) molecule is considered, the N- and C-terminal moieties are in positions 1 and 40, respectively

Position	*Acid*	*Position*	*Acid*	*Position*	*Acid*
1	Asp	6	His	11	Glu
2	Ala	7	Asp	12	Val
3	Glu	8	Ser	13	His
4	Phe	9	Gly	14	His
5	Arg	10	Tyr	15	GlN
16	Lys	21	Ala	26	Ser
17	Leu	22	Glu	27	Trp
18	Val	23	Asp	28	Lys
19	Phe	24	Val	29	Gly
20	Phe	25	Gly	30	Ala
31	Ile	36	Val	41	Ile
32	Ile	37	Gly	42	Ala
33	Gly	38	Gly	43	Thr
34	Leu	39	Val		
35	Met	40	Val		

TABLE II Comparison of the conformations* of A2OPT obtained by NMR and geometry optimization ($\varepsilon = 1$)

Source	*Sequence of amino acids of Aβ(1-40)* DAEFRHDSGYEVHHQKLVFFAEDVGSNKGAIIGLMVGGVV**
NMR	rrrhalaahahhrrhrhhhrrhhhllharhhhhhhhhlrr
Geometry-optimized	rrrrplaphahhrrhhhhhhhhhhhrlhprhhhhhhhhlrh

*Notations: r = random coil, h = right-hand helix, a = antiparallel β-sheet, l = left-hand α-helix, p = parallel β-sheet.
**Code of the amino acids see Table I.

similarity of a number of known structures and conformations. The standard geometry of each type of configuration is defined by the ϕ and ψ torsional angles of residues at the i and $(i+1)$ positions [24–27]. Due to environment-dependent variations in amino acid residues, the sequence of amino acids, and hydrogen-bonding forces, the torsional angles can vary statistically within the range of $\pm$ 30 degree [27].

Monomeric Aβ Peptides

The most known helix is the (right-hand) α-helix (abbreviated as "alpha" for simplicity). The left-hand a-helix is called "left". 3_{10}-helices ("310") are less frequently found in proteins and also referred to be a special type of type I β-turns (the other subtypes of β-turns are here not considered). Parallel β-sheets are abbreviated as "parall", and antiparallel β-sheets are called "anti". The double-C7 chair of the γ-turn is frequently referred as π-helix ("pi"). The extended γ-turn is abbreviated as "extend". A stochastic coil ("random") was designed by Monte Carlo technique. The Aβ(1-40) peptide contains many polar residues, which allow it to stabilize bulk water (in particular, at $\varepsilon = 80$) and charged reaction intermediates with membrane components, such as lecithin ($\varepsilon = 130$).

Within the different dielectric constants of the individual molecules, the total energies vary considerably, mainly due to the change of the electrostatic energies (Tab. III). Electrostatic interactions are strongly reduced in water and a lecithin-like environment, compared to vacuum and apolar conditions.

The α-helix has the lowest total energy values within the forgiven ranges of ε, followed by A2OPT and the unordered random-coil conformation. In particular, in water and blood plasma ($\varepsilon = 80$), the generally more stable α-helix, A2OPT and random-coil conformations dominate. In contrast, the total energy levels of the extended γ-turn and of the two β-sheets are large

in a polar ($\varepsilon = 80$) and lecithin-like environment ($\varepsilon = 130$), compared to the other conformations. For exemplary purpose, the conformations obtained in a lecithin-like environment are illustrated in Figures 1–9.

The stronger local energy minimum of the random coil and α-helix means that the two conformations are more stable in solution. Also, other water-soluble polymers undergo a significant conformational change from collapsed

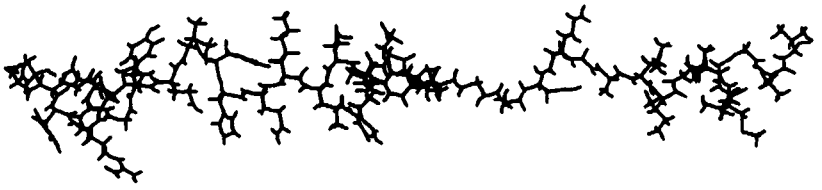

FIGURE 1 Geometry-optimized conformation of the 3_{10}-helix of Aβ(1-40) obtained in a lecithin-like environment ($\varepsilon = 130$).

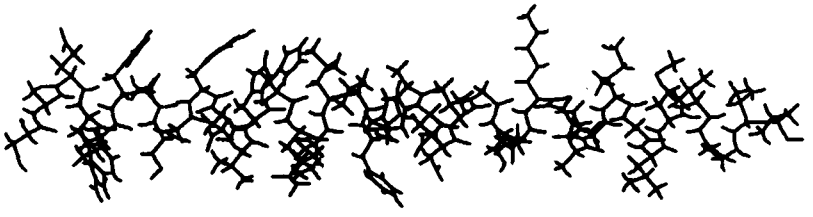

FIGURE 2 Geometry-optimized conformation of the right-hand α-helix of Aβ-(1-40) obtained in a lecithin-like environment ($\varepsilon = 130$).

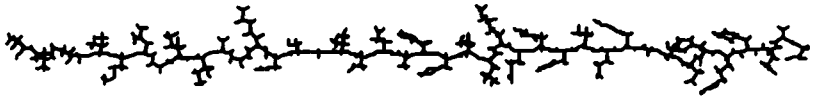

FIGURE 3 Geometry-optimized conformation of the antiparallel β-sheet of Aβ(1-40) obtained in a lecithin-like environment ($\varepsilon = 130$).

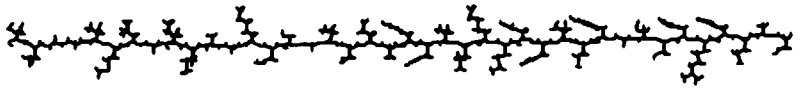

FIGURE 4 Geometry-optimized conformation of the extended γ-turn of Aβ(1-40) obtained in a lecithin-like environment ($\varepsilon = 130$).

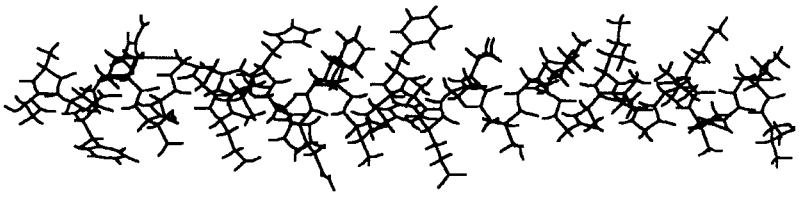

FIGURE 5 Geometry-optimized conformation of the left-hand α-helix of Aβ(1-40) obtained in a lecithin-like environment ($\varepsilon = 130$).

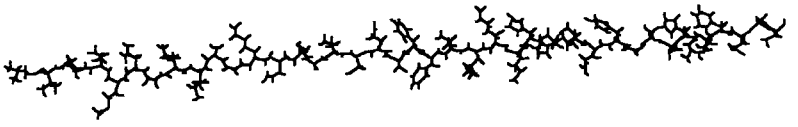

FIGURE 6 Geometry-optimized conformation of the parallel β-sheet of Aβ(1-40) obtained in a lecithin-like environment ($\varepsilon = 130$).

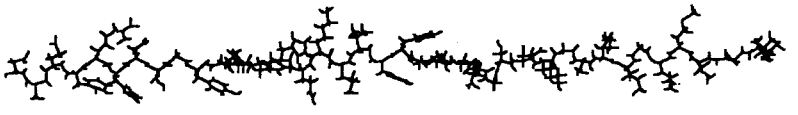

FIGURE 7 Geometry-optimized conformation of the π-helix of Aβ(1-40) obtained in a lecithin-like environment ($\varepsilon = 130$).

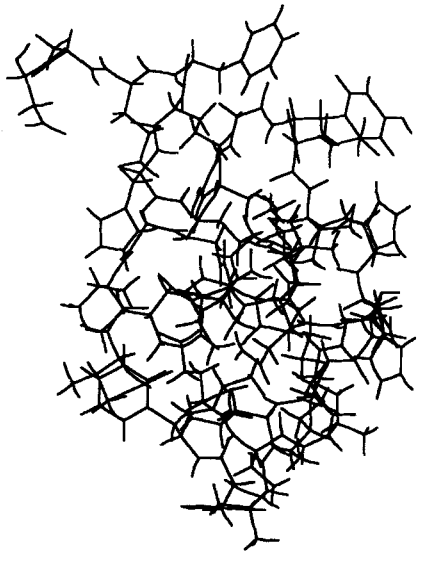

FIGURE 8 Geometry-optimized conformation of an unordered random coil of Aβ(1-40) obtained in a lecithin-like environment ($\varepsilon = 130$).

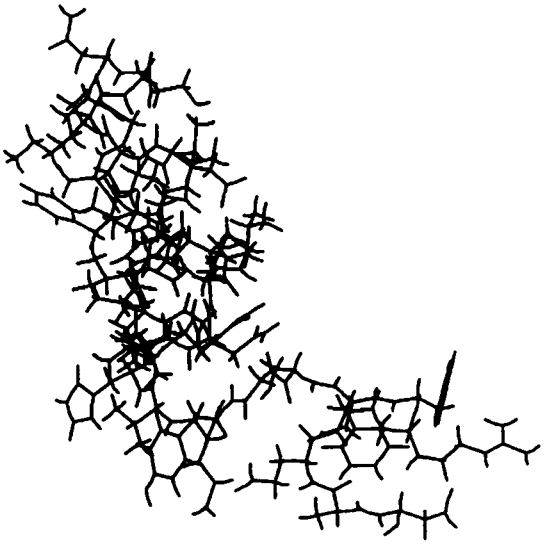

FIGURE 9 Geometry-optimized conformation of A2OPT (taken as file 1AML from PDB) of Aβ(1-40) obtained in a lecithin-like environment ($\varepsilon = 130$).

chains in vacuum and gas phase conditions, to an α-helix in water [38]. This agrees with the hypothesis that Aβ(1-40) is mainly transported in the blood in an α-helical conformation [28].

The relatively high-energy domain of the β-sheets allows to surmount better the energy-barrier height during the formation of an activated complex with polarized ligands and polarized macromolecules, such as lecithin, sphingomyelines, cerebrosides, and with other β-sheets of Aβ (di-, tri-, and oligomers). In contrast, the formation of paired helical Aβ peptides would be energetically unfavorable compared to the formation of paired β-sheets.

The usefulness of cluster analysis in molecular simulation studies was demonstrated quite recently; the following descriptors were used: canonical correlation coefficients of Cartesian coordinates [34], torsional angles [35,36], atomic distances [35], subsets of atoms [37], and energies [35]. Here, the relative energies (Tab. III) were used in dependence on the chosen dielectric ε constants, and analyzed by hierarchical cluster analysis (Euclidean distance, Ward linkage). Table IV gives the complete results, and Figure 10 illustrates an example of a cluster tree.

With respect to $\varepsilon = 1$, 3.5 to 39.65, strong similarities of the energetic profile exist between the antiparallel and parallel β-sheets which are both

TABLE III Relative energies (kcal/mol) of the geometry-optimized low-energy conformations of Aβ(1-40). After geometry optimization using the Gasteiger-MM+ approach, subsequent geometry optimization was applied using the AMBER force field model. Abbreviations of the structures see text, ε = dielectric constant, vdW = van-der-Waals energy

		Energies (kcal/mol)						
Structure	ε	*total*	*bonds*	*angles*	*dihedral*	*vdW*	*H-bond*	*Coulomb*
310	1	−224.61	4.32	76.29	15.50	−92.18	−8.70	−219.85
	3.5	−69.35	4.41	76.15	15.30	−95.47	−7.90	−61.85
	39.65	−13.06	4.51	76.44	15.32	−96.09	−7.79	−5.45
	80	−10.30	4.52	76.45	15.33	−96.11	−7.79	−2.70
	130	−9.26	4.52	76.45	15.33	−96.11	−7.79	−1.66
alpha	1	−302.43	4.35	74.56	15.55	−134.41	−18.22	−244.26
	3.5	−128.75	4.57	75.28	15.65	−136.98	−17.98	−69.30
	39.65	−65.62	4.59	75.66	15.66	−137.48	−17.96	−6.11
	80	−62.54	4.60	75.67	15.67	−137.50	−17.96	−3.03
	130	−61.38	4.59	75.67	15.67	−137.50	−17.96	−1.68
anti	1	−167.63	4.09	74.69	18.12	−42.91	−9.05	−212.59
	3.5	−17.30	4.14	74.49	17.67	−45.46	−8.06	−60.08
	39.65	37.40	4.18	74.65	17.68	−45.89	−7.93	−5.29
	80	40.07	4.18	74.66	17.68	−45.90	−7.93	−2.62
	130	41.08	4.19	74.66	17.68	−45.90	−7.93	−1.61
extend	1	−156.17	4.33	75.02	14.33	−27.21	−10.59	−212.05
	3.5	−5.54	4.61	74.41	14.55	−29.49	−9.63	−56.00
	39.65	49.09	4.60	74.48	14.51	−29.74	−9.48	−5.29
	80	51.74	4.61	74.53	14.51	−29.86	−9.44	−2.62
	130	52.74	4.61	74.53	14.50	−29.86	−9.44	−1.61
left	1	−255.28	6.77	100.16	16.75	−121.55	−20.14	−237.09
	3.5	−87.45	7.10	99.66	16.26	−123.85	−20.16	−66.77
	39.65	−26.70	7.28	100.24	16.27	−124.50	−20.12	−5.88
	80	−23.78	7.39	100.37	16.25	−124.74	−20.14	−2.91
	130	22.66	7.39	100.37	16.25	−124.74	−20.14	−1.79

TABLE III (Continued)

		Energies (kcal/mol)						
Structure	*ε*	*total*	*bonds*	*angles*	*dihedral*	*vdW*	*H-bond*	*Coulomb*
parall	1	−176.49	4.75	75.71	14.44	−45.88	−8.53	−216.97
	3.5	−22.80	4.68	75.78	13.94	−48.24	−7.63	−61.33
	39.65	33.05	4.72	75.97	13.94	−48.65	−7.54	−5.40
	80	35.77	4.72	75.98	13.95	−48.66	−7.53	−2.68
	130	36.81	4.72	75.98	13.95	−48.66	−7.53	−1.65
pi	1	−187.84	4.53	80.05	17.13	−56.00	−11.29	−222.27
	3.5	−31.50	4.57	79.96	16.58	−60.28	−9.67	−62.66
	39.65	25.58	4.58	80.05	16.57	−60.53	−9.58	−5.52
	80	28.39	4.63	80.21	16.60	−60.86	−9.51	−2.74
	130	29.39	4.63	80.21	16.60	−60.86	−9.51	−1.68
random	1	−244.10	5.67	91.82	25.52	−144.12	−9.12	−213.87
	3.5	−99.08	5.95	92.11	26.64	−156.27	−7.76	−59.75
	39.65	−46.03	5.94	92.28	26.24	−157.71	−7.54	−5.24
	80	−43.39	5.94	92.30	26.25	−157.76	−7.52	−2.60
	130	−42.39	5.94	92.25	26.25	−157.76	−7.52	−1.60
A2OPT	1	−289.76	4.89	78.78	16.95	−140.10	−11.98	−238.30
	3.5	−120.81	5.10	79.26	16.19	−142.72	−11.49	−67.15
	39.65	−59.71	5.30	79.79	16.19	−143.67	−11.39	−5.91
	80	−43.39	5.94	92.30	26.25	−157.76	−7.52	−2.56
	130	−42.39	5.94	92.30	26.25	−157.76	−7.52	−1.60

TABLE IV Compared conformation pairs (*P*)*, Euclidean distances (*D*) obtained by the energy data of Table II, and assignment to clusters (*Cl*)

$\varepsilon = 1.00$			$\varepsilon = 3.50$			$\varepsilon = 39.65$			$\varepsilon = 80.00$			$\varepsilon = 130.00$		
P	*D*	*Cl*	*P*	*D*	*Cl*	*P*	*D*	*Cl*	*P*	*D*	*Cl*	*P*	*D*	*Cl*
3, 6	4.17	2	3, 6	2.82	2	3, 6	2.47	2	8, 9	0.015	2	8, 9	0.019	2
2, 9	6.41	2	2, 9	4.77	2	2, 9	4.38	2	3, 6	2.46	2	3, 6	2.45	2
6, 7	9.47	3	6, 7	8.08	3	6, 7	7.50	3	6, 7	7.60	3	6, 7	7.60	3
4, 6	14.09	4	4, 6	13.50	4	4, 6	12.95	4	4, 6	12.93	4	4, 6	12.93	4
5, 8	14.36	2	5, 8	14.91	2	8, 9	13.39	3	2, 9	15.59	3	2, 9	15.55	3
1, 8	22.98	3	1, 8	19.99	3	1, 5	15.68	2	1, 5	15.74	2	1, 5	19.17	2
8, 9	36.16	5	8, 9	29.20	5	5, 8	30.60	5	5, 9	30.86	5	5, 9	40.48	5
6, 8	99.47	9	6, 8	94.51	9	5, 6	92.94	9	5, 6	83.28	9	5, 6	88.76	9

*1 = 3_{10} helix, 2 = right-hand α-helix, 3 = antiparallel β-sheet, 4 = extended γ-turn, 5 = left-hand α-helix, 6 = parallel β-sheet, 7 = π-helix, 8 = random coil, 9 = A2OPT.

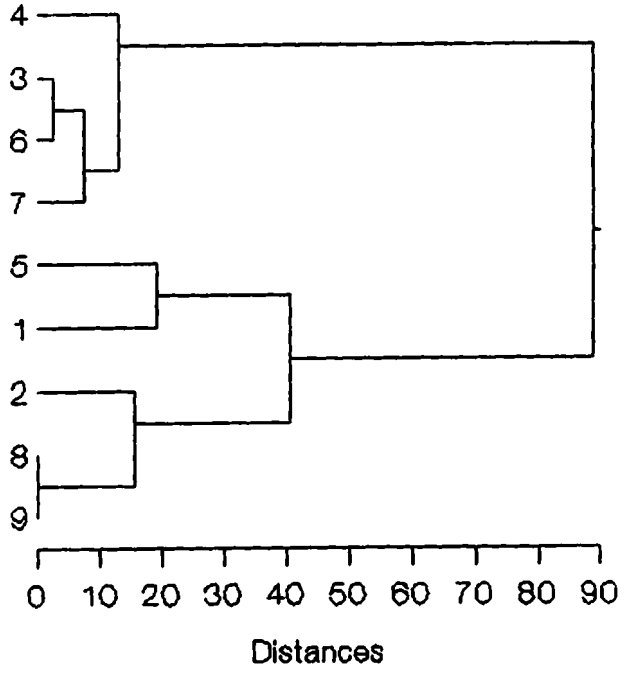

FIGURE 10 Example of hierarchical cluster analysis (Euclidean distance, Ward linkage) applied to the various energy-minimum optimized geometries of Aβ(1-40) using a lecithin-like environment ($\varepsilon = 130$).

associated with the π-helix and extended γ-turn. Similarities exists also between the (right-hand) α-helix and A2OPT conformation which are both not associated with the random-coil conformation.

With respect to $\varepsilon = 80$ and 130, strong energetic similarities exist between the antiparallel and parallel β-sheets which are both associated with the π-helix and extended γ-turn. Furthermore, strong similarities existed between the A2OPT conformation and random coil which are both associated with the (right) α-helix.

The hypothesis of energetically based transitions of Aβ conformations is supported by the experimental finding [7,28] that the Aβ peptides adapt coexisting mixtures of conformations in solutions, namely of random coils, α-helices, and β-sheets where the relative ratios are influenced by aging of the preparation and environmental conditions (concentration of the peptide, ionic strength, *p*H, temperature).

To investigate the physicochemical properties, the surface area (*SA*), molar volume (*MV*), hydration energy ΔH (kcal/mol), molefraction (*MR*), polarizability (*Pol*), and distribution coefficients (expressed as log*P*) were determined (Tabs. V and VI). It can be seen that the random coil, α-helix and A2OPT conformation have the smallest surface and volume. Furthermore, the absolute values of the hydration energy are low, in particular, with respect to the random coil and α-helix.

As the *p*H of the brain from patients with Alzheimer disease [38] is 6.6, the corresponding distribution coefficients are of particular interest. The results agree with the experimental finding [28,39] that the (i) the monomeric, purified Aβ peptides are soluble in water, (ii) degree of solubility depends on the *p*H, (iii) C-terminal amino acids are relatively less hydrophilic than the amino acids at the N-terminus, and (iv) hydrophilicity of the N-terminus depends more strongly on the *p*H of the tissues than the reduced hydrophilicity of the C-terminus.

TABLE V Physicochemical parameters of the various geometry-optimized. low-energy conformations (exemplified for $\varepsilon = 1$) of Aβ(1-40): Surface area *SA* (grid, Å^2), molar volume *MV* (Å^3), and hydration energy ΔE (kcal/mol). The molrefraction $MR = 1054.48$ Å^3 and polarizability $Pol = 428.89$ Å^3 are calculated independently on geometry optimization

Code	*SA*	*MV*	ΔE
310	4775.67	10462.85	−108.00
alpha	4224.96	9938.98	−96.97
anti	5682.01	11308.28	−130.44
extend	5818.77	11346.65	−128.52
left	4089.26	9863.06	−93.70
parall	5502.65	11083.91	−120.56
pi	5193.01	10751.09	−116.28
random	3196.70	8999.53	−96.45

TABLE VI Distribution coefficients P (octanol/water, expressed as log$P$ values) of synthetic Aβ(1-14) to Aβ(30-43) peptides that represent distinct regions of the Aβ peptide

	pH values							
Peptide	1.0	2.0	5.0	6.0	6.6	7.0	7.4	8.0
1–14	−18.72	−18.61	−13.62	−12.89	−12.89	−13.30	−13.46	−14.0
15–29	−12.85	−12.25	−9.14	−8.23	−7.69	−7.33	−7.08	−6.9
30–39	−3.72	−3.68	−3.42	−2.70	−3.03	−2.38	−2.36	−1.9
30–40	−2.64	−2.64	−2.62	−2.50	−2.25	−1.99	−1.68	−1.2
30–43	−1.96	−1.45	−1.33	−1.33	−1.34	−1.35	−1.39	−1.5

In analogy to the rules of drug transport [40], the results (steric parameters, hydrophilicity) support the hypothesis that the various Aβ(1-40) peptides are transported through membranes and in the plasma. In particular, the energetically more stable α-helix and random coil-conformation may be transported in the blood stream [28].

Marginal Remark

It was stated [4] that there is an unusual *cis* amide bond at the Gly37-Gly38 junction which is required for nucleation of the amyloid. In the studied peptides, we found the more stable *trans* amide bond independently on the type of conformation and solvation conditions.

Oligomeric Aβ Peptide

To simulate the process of crystallization, two and three geometry-optimized antiparallel β-sheets ($\varepsilon = 130$) were aggregated by molecular simulation. The structures were positioned in opposite directions by vector mapping. Then, presumed turned positions were conformationally restricted by the introduction of chargeless and dimensionless "dummy atoms" between the β-sheets. Initially, a distance of about 8 Å was used. In the next step, the minimum energy of the complex, and the distances and angles were calculated until the data were physically acceptable. The dummies were then omitted again, and the low-energy conformation was determined. The result of two aggregated β-sheets is illustrated in Figures 11, and Table VII shows the relative total, van-der-Waals, and hydrogen-bonding energies (AMBER force field) of the mono-, di-, and trimer (not illustrated here). In this lecithin-like environment, the contribution of electrostatic energies is again very small.

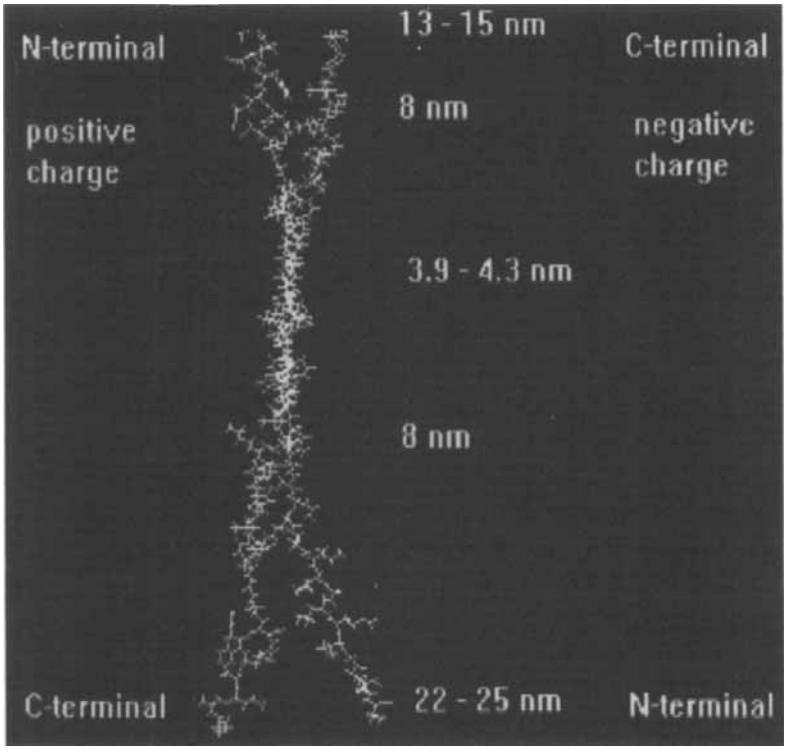

FIGURE 11 Geometry-optimized conformation of two antiparallel β-sheets of Aβ(1-40) obtained in a lecithin-like environment ($\varepsilon = 130$). After rotation of the paired molecule, a χ-like conformation can be observed (See Color Plate I).

It can be seen that the aggregated complexes are *thermodynamically* very stable, compared to the results obtained by a single β-sheet. Intra- and intermolecular interactions of the filamentous-like aggregates are mainly based on π-π, σ-σ and π-σ bonding forces [41] (van-der-Waals interactions as sum of dispersion and repulsion energies, hydrogen bonds, London forces, and hydrophobic bonds; the role of "pure" electrostatic interactions is solvent-dependent). An example of the molecular interactions is illustrated in Figure 12. It appears that hydrophobic interactions of an area around the Phe19 and Phe20 residues play a key role. This molecular simulation result agrees with the experimentally based hypothesis [39] that the size which is mainly responsible for filament formation is located from Leu17 to Ala 21 ("hydrophobic core") with distances of 3.5 to 5 Å. The dimer has a length of 125 to 130 Å. The maximum distances of

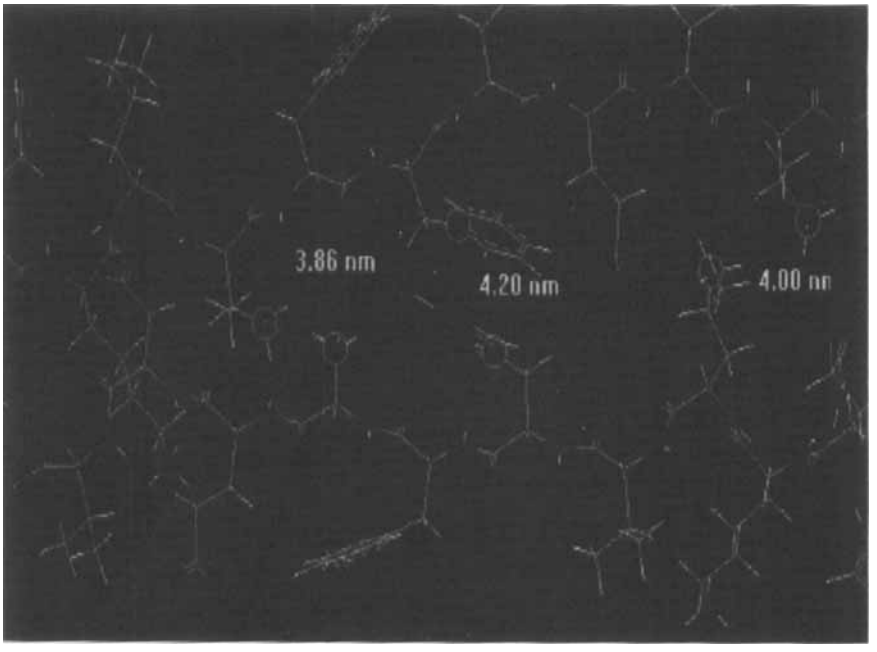

FIGURE 12 Example of molecular binding forces obtained in a lecithin-like environment ($\varepsilon = 130$) (See Color Plate II).

the paired amino acids at the C- and N-terminus are 13 to 15 and 22 to 25 Å, respectively. The graphics shows that a χ-like conformation of the dimer exists (Fig. 11).

Molecular dynamics is now used to examine the hypothesis that the α-helix is also energetically more stable than the antiparallel β-sheet after an input of energy. Figure 13 shows the change of total energy if it is assumed that the two conformations of Aβ(1-40) are in a fairly high-energy domain. It can be seen that the α-helix is "more resistant" to a rapid and strong input of temperature (Tab. VIII). Also, the percentage of changed conformations of amino acids is less than that of the β-sheet (Tab. VIII). In contrast, once *kinetically* activated, the junction of the "hydrophobic core" of the dimer is disconnected. After cooling, the process is not reversible (Fig. 14) as expected from the theory of denaturation. However, it might be expected that the dimer will be more stable in preparations containing also a high concentration of other polyelectrolytes, such as lecithin, sphingomyelines, or cerebrosides.

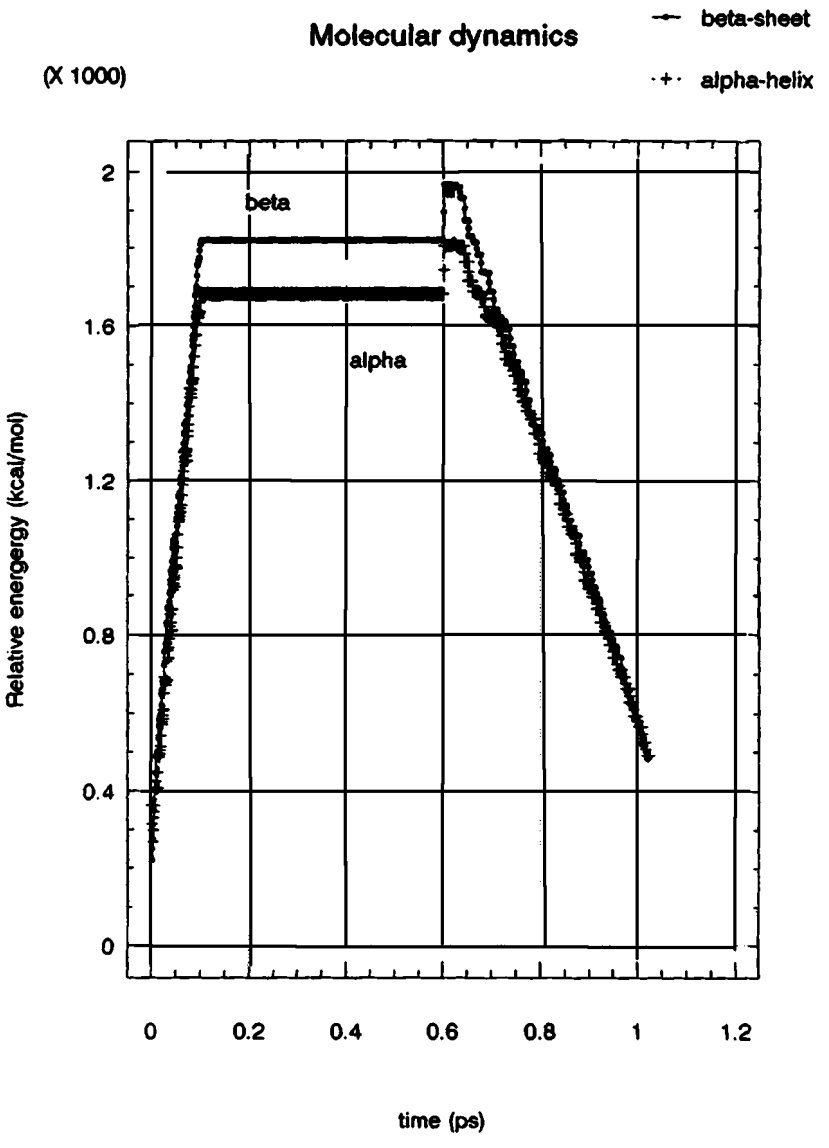

FIGURE 13 Result of the molecular dynamics study by MM+ applied to the Gasteiger-MM+/AMBER geometry-optimized structures ($\varepsilon = 130$) of the α-helix and β-sheet.

3. CONCLUSIONS AND FUTURE PERSPECTIVE

Aβ peptides can diffuse through membranes and transported in the blood plasma, either as a random-coil or α-helix conformation. The transition

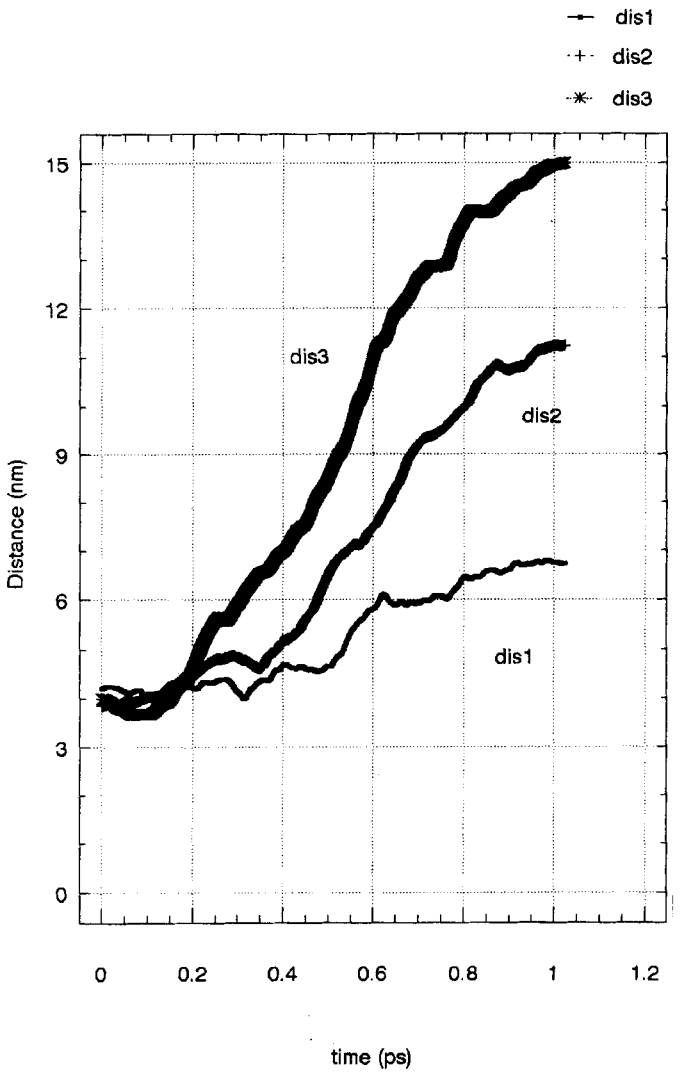

FIGURE 14 Result of the molecular dynamics study by MM+ applied to the Gasteiger-MM+/AMBER geometry-optimized structures (ε = 130) of the dimer. The three distances (dis1, dis2, dis3) were taken from Figure 13.

from an energetically more stable α-helix into a β-sheet is a prerequisite for filament formation. A hydrogen-bond breaking environment is required for this transition, however. The ability to form χ-like oligomers is mainly based on hydrophobic interactions around the area of the paired Phe19 and Phe20 residues, that is, the hydrophobic core would not extend through the

TABLE VII Relative energies (kcal/mol) of the geometry-optimized low-energy conformation of $A\beta(1\text{-}40)_n$ of the antiparallel β-sheet at $\varepsilon = 130$. After geometry optimization using the Gasteiger-MM+ approach, subsequent geometry optimization was applied using the AMBER force field model (*vdW* = van-der-Waals energy, *RMS* = root mean square)

		Energies (kcal/mol)		
n	*RMS*	*total*	*vdW*	*H-bond*
1	0.07	41.08	−45.90	−7.93
2	0.07	−101.69	−151.67	−18.22
3	0.13	−264.44	−374.43	−80.01

TABLE VIII Molecular dynamics by MM+ applied to Gasteiger/MM+/AMBER ($\varepsilon = 130$) geometry-optimized structures. Temperatures in Kelvin degree

Notation	*Primary structure** DAEFRHDSGYEVHHQKLVFFAEDVGSNKGAIIGLMVGGVV**	%
α-helix		
Temperatures		
100.00	rhhhhhhhhhhhhhhhhhhhhhhhhhhhhhhhhhhhhhh	98
522.10	rhhhrhhhhhrrhhrhhhrhhhhhrhhrrhrrrrhrrrrh	58
540.63	rhhrhhehhhrrhhrrhhrrhhhhhhhrrhhrrrrhhrrrh	58
534.69	hhhrrhhhhhrrrhhrrherrhhhhhhhrrhhrrrhhrrrr	55
487.95	rrrrhrhhrrrrhhrrheprhhhrhrhrrhhrrrhhrrrr	38
366.51	rrrrhrrhrrrhhhrrhhirhhhhhrhhrrhrrrrhhrhpr	38
antiparallel β-sheet		
Temperatures		
99.93	rprpaaaaraaaaaraaapaaxrarrxaaarpapprrrar	50
531.58	rrprphrarxaaaarrararrrraraaarripaxrrrapx	33
536.93	rrprahrarraaaarrarprrrrrrapararpaxrrrapr	30
560.21	rrpaphrxrraaarrrararrrrarapxrapraxrpappr	28
482.45	rrpaprlalaaaarhrarpraaraaaaarapparrprppr	40
363.43	rrppphlalppaaarrarpaparaaapalrarrrapprppr	30
random coil		
Temperatures		
100.00	rrahrrhrrarrrlrrhrrrrlrrrrrllhrhrphrrrpr	65
508.63	rhrrhrrarrrrrlhrxrrrhrlrraprrahrrrhprrar	63
527.14	rhrhrrrrrrrrrlhrrrrrrrlrraprrahrrphprrar	68
508.36	rrrhrrrrrrrrrlhrrrrrrrlrraprrrherphprrar	73
490.56	rrrhrrrrrhrrhlhrrrrrrrrlrrpprrrhrrrrarrar	73
366.14	rrrrrrrhrhrrhlhrrrrxrrllrrprrrrhrrphpprar	63

*h = (right-hand) α-helix, a = antiparallel β-sheet, r = random coil, e = 3_{10}-helix, l = left-hand α-helix, x = extended β-sheet, p = parallel β-sheet.
**Code of the amino acids see Table I.

whole length of the paired β-sheets. The resulting aggregates are thermodynamically but not kinetically stable. The resulting model is summarized in a Scheme.

UNTOXIC, LOW-ENERGY CONFORMATIONS OF Aβ(1-40) AND Aβ(1-42)
(monomeric, soluble structures)

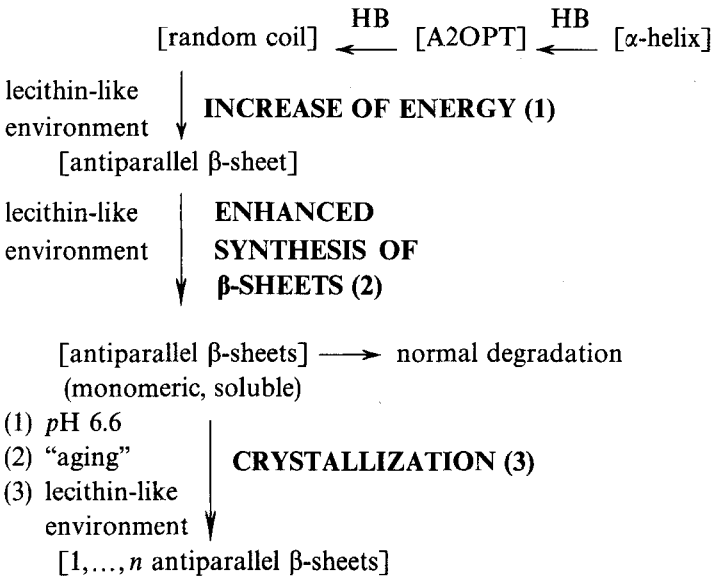

= TOXIC, LOW-ENERGY CONFORMATIONS OF Aβ $(1\text{-}40)_n$ AND Aβ$(1\text{-}42)_n$
(polymeric, unsoluble, extremely stable aggregates connected by π-π, σ-σ, and π-σ bonds)

SCHEME Model of the formation of aggregated β-sheets (HB = hydrogen-breaking solvent). In the *first phase*, conformational transition from an α-helix (transport through blood stream and membranes) to a β-sheet occurs with the consequence that the energy-barrier height of a binding to polar macromolecules (for example, lecithin-like structures) is surmounted. A hydrogen-breaking solvent is required. In the *second phase*, an enhanced synthesis of monomeric β-sheets is hypothesized. In the irreversible *third phase*, trace amounts of β-sheets that are bound with polar macromolecules, form a nucleus. This event depends on the time ("aging" of the solution). Once the core is formed, growth of polymeric Aβ$(1\text{-}40)_n$ and Aβ$(1\text{-}42)_n$ is fast [4]. One of the factors that facilitate the aggregation process is the *p*H of the "Alzheimer tissue" (*p*H = 6.6).

A furture perspective in drug research is to develop compounds that stabilize *selectively* the α-helix and random conformations of the Aβ-(1-40) and Aβ(1-42) peptides, and that inhibit aggregation by inhibition of the hydrophobic cores of paired β-sheets. An example of α-helix stabilizing agents is 1,1,1,3,3,3-hexafluoroisopropanol but this lead structure must be manipulated chemically to get a safer agent. An unsuccessful attempt would be to disrupt the complexed β-sheet structures.

Additional Material

The geometry-optimized conformations can be uploaded in PDB file format (*host* pharma.phto uni-leipzig.de, *login* pharma/guest, *directory* alzheim, *file names* '*_ε.ent where "*" denotes the code of the conformations of Aβ(1-40) defined in Table III and the text, and ε is the chosen dielectric constant.

Acknowledgement

I thank the technical assistance of Horst Walter, Monika Bretschneider, and Rosemarie Wolfram.

References

[1] Selkoe, D. J. (1994). "Normal and Abnormal Biology of the β-Amyloid Precursor Protein", *Ann. Rev. Neurosci.*, **17**, 489–517.
[2] Kang, J., Lemaire, H. G., Unterbeck, A., Salbaum, J. M., Masters, C. L., Grzeschik, K. H., Multhaup, G., Beyreuther, K. and Müller-Hill, B. "The Precursor of Alzheimer's Disease Amyloid A4 Protein Resembles a Cell-surface Receptor", *Nature*, **325**, 733–736.
[3] Krafft, G. (1993). "Prespectives on Amyloid and Alzheimer's Disease: a Critical Review", *Ann. Rep. Med. Chem.*, **28**, 49–58.
[4] Jarrett, J. T., Berger, E. P. and Lansburg, P. T. Jr. (1993). "The Carboxy Terminus of the β Amyloid Protein is Critical for the Seeding of Amyloid Formation: Implications for the Pathogenesis of Alzheimer's Disease", *Biochemistry*, **32**, 4693–4697.
[5] Mori, H., Takio, K., Ogawara, M. and Selkoe, D. J. (1992). "Mass Spectrometry of Purified Amyloid β Protein in Alzheimer's Disease", *Biol. Chem.*, **267**, 17082–17806.
[6] Prelli, F., Castano, E. M., van Duinen, S. G., Bots, G. T. A. M., Luyendijk, W. and Frangione, B. (1988). "Differential Processing of Alzheimer's β-protein Precursor in the Vessel Wall of patients with Hereditary Cerebral Hemorrhage with Amyloidosis-Dutch Type", *Biochem. Biophys. Res. Commun.*, **151**, 1150–1155.
[7] Simmonis, L. W., May, P. C., Tomaselli, K. J., Reydel, R. E., Fuson, K. S., Brigham, E. F., Wright, S., Lieberburg, I., Becker, G. W., Brems, D. N. and Li, W. Y. (1994). "Secondary Structure of Amyloid β Peptide Correlates with Neurotoxic Activity *in vitro*", *Mol. Pharmacol.*, **45**, 373–379.
[8] Williams, M., Shiosaki, K. and Puttfarcken, P. (1995). "Amyloid β Peptide in Alzheimer's Disease Pathology: Towards a Rational Basis for Drug Discovery?", *Exp. Opin. Invest. Drugs*, **4**, 263–270.
[9] Maeda, H., Gatto, Y. and Ikeda, S. (1984). "Effects of Chain Length and Concentration of the β-Coil Conversion of Poly[S-carboxymethyl)-L-cysteine] in 50 nM NaCl solution", *Macromolecules*, **17**, 2031–2037.
[10] Kanô, F. and Maeda, H. (1996). "Monte Carlo Simulation of the β-sheet-Random Coil Transition of a Homopolypeptide", I. Equilibrium Study. *Mol. Simul.*, **16**, 261–274.
[11] Kemp, D. S., Allen, T. J. and Ostlick, S. L. (1995). "The Energetics of Helix Formation by Short-Templated Peptides in Aqueous Solution. 1. Characterization of the Reporting Helical Template Ac-Hel$_1$", *J. Am. Chem. Soc.*, **117**, 6641–6657.
[12] Perderson, D., Gabriel, D. and Hermans, J. Jr. (1971). "Potentiometric Titration of Poly-L-lysins: the Coil-to-β Transition", *Biopolymers*, **10**, 2133–2145.
[13] Kanô, F. (1976). "Theory of the Phase Transition Between the Intra β-Structure and the Random Coil in Polyamino Chains", *J. Phys. Soc. Jp.*, **41**, 219–227.
[14] Wakana, H., Shigaki, T. and Saitô, N. (1982). "Intramolecular α-Helix/β-Structure/Random Coil Transition in Polypeptides. I. Equilibrium Case", *Biphys. Chem.*, **16**, 275–285.

[15] Mattice, W. L. and Scheraga, H. A. (1984). "Matrix Formulation of the Transition from a Statistical Coil to an Intramolecular Antiparallel β Sheet", *Biopolymers*, **24**, 1701–1724.
[16] Mattice, W. L. and Scheraga, H. A. (1985). "Role of Interstrand Loops in the Formation of Intramolecular Cross-β-sheets by Homopolyamino Acids", *Biopolymers*, **24**, 565–579.
[17] Mattice, W. L. (1989). "The β-Sheet to Coil Transition", *Annu. Rev. Biophys. Biochem.*, **18**, 93–111.
[18] Allinger, N. L. and Yan, L. (1993). "Molecular Mechanics (MM3). Calculation of Furan, Vinyl, Ethers, and Related Compounds", *J. Am. Chem. Soc.*, **115**, 11918–11925.
[19] Tai, J. C., Yang, L. and Allinger, N. L. (1993). "Molecular Mechanics (MM3). Calculation on Nitrogen-Containing Aromatic Heterocyclics", *J. Am. Chem. Soc.*, **115**, 11906–11917.
[20] Weiner, S. J., Kollman, P. A., Nguyen, D. T. and Case, D. A. (1986). "An All Atom Force Field for Simulations of Proteins and Nucleic Acids", *J. Comput. Chem.*, **7**, 230–252.
[21] Frey, R. F., Coffin, J., Newton, S. Q., Ramek, M., Cheng, V. K. W., Momany, F. A. and Schäfer, L. (1992). "Importance of Correlation-Gradient Geometry Optimization for Molecular Conformational Analyses", *J. Am. Chem. Soc.*, **114**, 5369–5377.
[22] Gasteiger, J. and Marsili, M. (1980). "Iterative Partial Equalization of Orbital Electronegativity – a Rapid Access to Atomic Charges", *Tetrahedron*, **36**, 3219–3288.
[23] Brookhaven Protein Data Bank (PDB), files 1AML [Aβ(1-40), Febr. 13, 1995] and 1AMB [(Aβ(1-28), Oct 21, 1994], with physical details of experimental determination.
[24] Venkatachalam, C. M. (1968). "Stereochemical Criteria for Polypeptides and Proteins. V. Conformation of a System of Three Linked Peptide Units", *Biopolymers*, **6**, 1425–1436.
[25] Perczel, A., McAllister, M. A., Császár, P. and Czizmadia, I. G. (1993). "Peptide Models. 6. New β-Turn Conformations from *ab initio* Calculations Confirmed by X-Ray Data of Proteins", *J. Am. Chem. Soc.*, **155**, 4849–4858.
[26] Böhm, H.-J. (1993). "*Ab initio* SCF Calculations on Low-Energy Conformers of N-Acetylglycine *N'*-Methylamide", *J. Am. Chem. Soc.*, **115**, 6152–6158.
[27] Xie, P., Zhou, O. and Diem, M. (1995). "Conformational Studies on β-Turns in Cyclic Peptides by vibrational CD", *J. Am. Chem. Soc.*, **117**, 9502–9508.
[28] Barrow, C. J., Ykikazu, A., Kenny, P. T. M. and Zagorski, M. G. (1992). "Solution Conformations and Aggregational Properties of Synthetic Amyloid β-Peptides of Alzheimer's Disease", *J. Mol. Biol.*, **225**, 1075–1093.
[29] Eisenhaber, F., Lijnzaad, P., Argos, P., Sander, C. and Scharf, M. (1995). The Double Cubic lattice Method: Efficient Approaches to Numerical Integration of Surface Area and Volume and to Dot Surface Contouring of Molecular Assemblies", *J. Comput. Chem.*, **16**, 273–284.
[30] Meylan, W. M. and Howard, P. H. (1995). "Atom/Fragment Contribution Method for Estimating Octanol-Water Partition Coefficients", *J. Pharm. Sci.*, **84**, 83–92.
[31] Stout, J. M. and Dykstra, C. E. (1995). "Static Dipole Polarizabilities and a Predictive Model", *J. Am. Chem. Soc.*, **117**, 5127–5132.
[32] Dixon, S. L. and Jurs, P. C. (1993). "Estimation of pK_a for Organic Oxyacids Using Calculated Atomic Charges", *J. Comput. Chem.*, **14**, 1460–1467.
[33] Pauling, L. (1970). "*General Chemistry*", W. H. Freeman and Co: San Francisco, p. 395.
[34] Mager, P. P. (1996). "Multivariate Investigations of Random-Coil and Ordered-Structure Conformations of the Tyr181-to-Tyr188 Segment of HIV-1 Reverse Transcriptase", *Mol. Simulation.*.
[35] Michel, A. G. and Jeandenans, C. "Multiconformational Investigations of Polypeptide Structures, Using Clustering Methods and Principal Components Analysis", *Computers Chem.*, **17**, 49–59.
[36] Shenkin, P. S. and McDonald, D. Q. (1994). "Cluster Analysis of Molecular Conformations", *J. Comput. Chem.*, **15**, 899–916.
[37] Torda, A. E. and van Gunsteren, W. F. (1994). "Algorithms for Clustering Molecular Dynamics Configurations", *J. Comput. Chem.*, **12**, 1331–1340.
[38] Yates, C. M., Butterworth, J., Tennant, M. C. and Gordon, A. (1990). "Enzyme Activation in Relation to *p*H and Lactate in Postmortem Brain in Alzheimer-type and Other Dementias", *J. Neurochem.*, **55**, 1624–1630.

[39] Hilbich, C., Kisters-Wolke, B., Reed, J., Masters, C. L. and Beyyreuther, K. (1991). "Aggregation and Secondary Structure of Synthetic Amyloid βA4 Peptide of Alzheimer's Disease", *J. Mol. Biol.*, **218**, 149–163.
[40] Palm, K., Luthman, K., Ungell, A.-L., Standlund, G. and Artursson, P. (1996). "Correlation of Drug Absorption with Molecular Surface Properties ", *J. Pharm. Sci.*, **85**, 32–39.
[41] Hunter, C. A. (1994). "The Role of Aromatic Interactions in Molecular Recognition", *Chem. Soc. Rev.*, 101–109.